


Cite this: *RSC Adv.*, 2020, 10, 10188

# Tetrahydropyrazolopyridines as antifriction and antiwear agents: experimental and DFT calculations†

Kavita,<sup>‡a</sup> Pratibha Verma,<sup>‡a</sup> Dinesh K. Verma,<sup>ab</sup> Bharat Kumar,<sup>a</sup> Alok K. Singh,<sup>a</sup> Nivedita Shukla,<sup>a</sup> Vandana Srivastava<sup>a</sup> and Rashmi B. Rastogi<sup>ib\*</sup>

Some tetrahydropyrazolopyridines (THPP-H) with the methoxy (THPP-OMe) and methyl (THPP-Me) substituents were synthesized by a one-pot multi-component reaction. NMR spectroscopy (<sup>1</sup>H and <sup>13</sup>C) was used to authenticate the synthesis. According to the results of tribological tests ASTM D4172, and ASTM D5183 on a four-ball tester in paraffin oil (PO) at a concentration of 0.25% w/v, their relative tribo-activity along with a reference additive, zinc dialkyldithiophosphate (ZDDP) could be figured out as mentioned below-THPP-OMe > THPP-Me > THPP-H > ZDDP. The calculation of frictional power loss from the coefficient of friction data of the tested additives supports the given order. As is apparent from AFM and SEM micrographs of the wear scar surface for plain oil with and without different tetrahydropyrazolopyridines, surface evenness endorses the above trend. Proof for strong adsorption of the synthesized additives is provided by EDX analysis of the steel ball surface after performing the tribological test, where nitrogen and oxygen are vividly seen as heteroatoms. XPS studies reveal the composition of the *in situ* formed tribofilm. The moieties containing carbon bonded to oxygen/nitrogen as decomposed products of the additive together with oxides of iron in +II or +III oxidation states are perceptible in the tribofilm, the tribofilm interferes with the proximity of the surfaces keeping them far apart. Consequently, friction and wear are remarkably reduced. Findings from Density Functional Theory (DFT) calculations are in full agreement with the results obtained from tribological experiments.

Received 26th January 2020  
Accepted 2nd March 2020

DOI: 10.1039/d0ra00794c

rsc.li/rsc-advances

## 1. Introduction

Friction and wear together have been immanent adversaries to mechanical systems. Lubrication stands as the only remedial measure to safeguard such systems.<sup>1–5</sup> Sundry lubricant systems with numerous types of additives, therefore, have been fabricated to address this issue. Among them, heterocyclic organic compounds,<sup>6</sup> nanomaterials,<sup>7,8</sup> inorganic lamellar structures<sup>9</sup> and metal complexes<sup>10</sup> find paramount significance. Zinc dialkyldithiophosphates (ZDDP) have been employed, very often, as multifaceted antiwear additives.<sup>11,12</sup> However, their incessant use is prohibited because of their susceptibility to attenuating the efficacy of exhaust emission catalytic converters, thus enhancing air pollution.<sup>13</sup> From an environmental perspective,

various standards have been put forth to control sulphated ash, sulphur and phosphorus (SAPS) contents in an additive.<sup>14</sup>

Nanolubricants<sup>15,16</sup> are well appreciated for their dexterous antiwear behavior but their agglomeration poses a great problem for the stability of their dispersions. In contrast, the use of conventional organic compounds is everlasting owing to their comparatively higher solubility in base oils. From the viewpoint of adsorption over the metal/alloy surface, heterocyclic compounds containing heteroatoms specifically, nitrogen and oxygen are categorically advocated for their friction/wear lowering disposition. The lone pair of electrons at heteroatoms and the aromatic ring electrons are basically involved in the process of adsorption.<sup>17–20</sup> A comprehensive literature survey reveals that several groups of workers have chosen to investigate the tribological efficiency of different types of heterocyclic compounds. Kamano *et al.* have patented several pyridines, pyridazines, pyrazines, pyrimidines, pyrroles, pyrazoles, imidazoles as antiwear agents.<sup>21</sup> Friction and wear-reducing behavior of indole, indazole and benzotriazole in liquid paraffin oil have been reported by Zhongyi and co-workers.<sup>22</sup> Tribological properties of the benzimidazoles<sup>23</sup> and tetrazole derivatives<sup>24</sup> have been investigated in liquid paraffin oil. The antiwear and antifriction properties of imidazoline derivatives<sup>25</sup> in water-glycol mixture and triazine in poly-alpha olefin base

<sup>a</sup>Department of Chemistry, Indian Institute of Technology (Banaras Hindu University), Varanasi-221005, India. E-mail: rashmi.apc@iitbhu.ac.in

<sup>b</sup>Department of Chemistry, Prof. Rajendra Singh (Rajju Bhaiya) Institute of Physical Sciences for Study & Research, V. B. S. Purvanchal University, Jaunpur-222003, U. P., India

† Electronic supplementary information (ESI) available. See DOI: 10.1039/d0ra00794c

‡ These authors contributed equally to this work.



oil<sup>26</sup> have been studied. Desanker *et al.* have tested the performance of alkyl-substituted cyclen derivative (commercial Group III lubricating oil) as friction modifier using pin-on-disk tribometry tests.<sup>27</sup> Several ionic liquids such as di[bis(2-hydroxyethyl)ammonium]succinate,<sup>28</sup> 1-acetyl-3-hexylbenzotriazolium benzoate/sorbate,<sup>29</sup> poly-alkylimidazoliumbis(trifluoromethylsulfonyl)imide,<sup>30</sup> alkylimidazolium diethyl phosphates,<sup>31</sup> bis(imidazolium)/bis(ammonium)-di[bis(salicylato)borate]<sup>32</sup> are reported as effective antiwear agents. Quinoline derivatives<sup>33</sup> in polyethylene glycol (PEG) and Schiff bases of 4-aminoantipyrine with substituted benzaldehyde<sup>34</sup> in paraffin oil have been reported as excellent tribological additives from our laboratory. There is always an urge to develop more and more superior antiwear additives of different types. This instigated us to synthesize substituted tetrahydropyrazolopyridines, having two pyrazoles and a pyridine ring arranged in a specific fashion and evaluate their tribological behavior in paraffin oil on a four-ball tribo-tester. The tribo-activity is directly related to the number of adsorption centres accessible to the metal surface. The adsorption of substituted tetrahydropyrazolopyridines on the steel surface is anticipated to occur primarily through the nitrogen atoms, provided these are competent enough to approach the surface. The inherent properties of the substituents at the pyridine ring may facilitate adsorption by enhancing electron density at these nitrogen atoms. For a deep insight into electronic environments around adsorption centres, Density Functional Theory calculations were also performed. These calculations have been used to validate the observed tribological results.

## 2. Experimental section

### 2.1. Chemicals

AR grade chemicals were utilized throughout the investigation.

### 2.2. Synthesis of tetrahydropyrazolopyridine derivatives

2.0 mmol hydrazine hydrate and 2.1 mmol ethyl acetoacetate in ethanol (5 mL) were taken in a round bottom flask. The reactants were stirred for half an hour at 30 °C and 1.0 mmol aldehyde and 4.0 mmol ammonium acetate were successively added. The prepared reaction mixture was refluxed for 4–8 h and then cooled to normal temperature. The distilled water (10 mL) was added, and the mixture was stirred for 30 min.<sup>35</sup> The resulting product was filtered, washed with distilled water followed by acetone and dried under vacuum (Scheme 1).

NMR spectroscopy was used to characterize the synthesized product. The <sup>1</sup>H and <sup>13</sup>C NMR spectra of the prepared additives have been provided in the ESI (ESI-1 Fig. S1–S6†). The IUPAC names, abbreviations, structures and characterization of the tetrahydropyrazolopyridines are given in (Table 1).

### 2.3. Tribological analysis

**2.3.1. Preparation of admixtures.** Tetrahydropyrazolopyridine blends in paraffin oil (base oil) with concentrations (0.00, 0.125, 0.25, 0.50, 0.75 and 1.0% w/v) were made by stirring at 40–50 °C for 1–2 hour followed by 1 h sonication at room temperature. The optimized concentration of the additives was

identified as 0.25% w/v. All tribological tests, therefore, were conducted at the concentration, 0.25% w/v.

Tribological testing procedures and surface analysis adopted in the present investigation were the same as reported from our laboratory<sup>5–8</sup> and are provided as the ESI (ESI-2†).

### 2.4. Computational details

DFT computations were performed with the help of B3LYP. Full geometry of the additives was optimized with the standard B3LYP/321G+\* basis set applying Gaussian 03, revision C. 01.<sup>36</sup>

## 3. Results and discussion

### 3.1. Antiwear studies

The antiwear tests of paraffin oil (PO) with or without synthesized tetrahydropyrazolopyridine derivatives were performed with the help of a four-ball tester. At first, the concentration of the additive was optimized. Fig. 1 displays the deviation in the mean wear scar diameter (MWD) against the concentration of the synthesized additives (0.00 to 1.0% w/v) in base lube at 392 N load for 60 minutes.

It is obvious from Fig. 1 that as compared to plain paraffin oil, the MWD decreases for its blends with tetrahydropyrazolopyridines at all the investigated concentrations up to 0.25% w/v. Beyond 0.25% w/v, there is a sluggish hike in MWD in every case up to 1% w/v. Although the additives are triboactive at all the tested concentrations, 0.25% w/v is considered as the optimum concentration for testing. It is important to point out here that in case of the commercial additive ZDDP, the MWD is much higher at 0.25% w/v and the minimum value is obtained at four times higher concentration, 1% w/v.

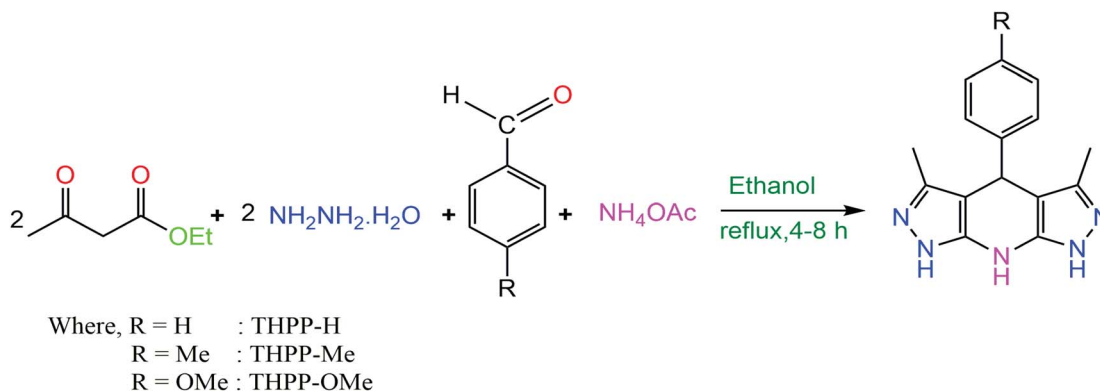
Fig. 2 exhibits how COF varies with time for paraffin oil and its admixtures with various tetrahydropyrazolopyridines for the optimized concentration (0.25% w/v) at load 392 N and 60 min duration.

As per figure, the highest diminution in the coefficient of friction values is noted for THPP-OMe followed by THPP-Me and finally THPP-H.

Fig. 3 displays magnitude of reduction in MWD and COF data simultaneously for base oil with or without the synthesized additives. The MWD for base oil (0.733 mm) undergoes about 21, 26 and 35% reduction in the presence of THPP-H, THPP-Me and THPP-OMe respectively. However, there is only an 11% reduction in MWD for the standard additive zinc dialkylthiophosphate (ZDDP). The observed data indicate the highest antiwear performance for the THPP-OMe derivative. Similarly, reduction in values of the coefficient of friction (COF) of base oil (0.0948) is observable in its blends with ZDDP (11%), THPP-H (13%), THPP-Me (26%) and THPP-OMe (40%) supporting the maximum antifriction performance again for THPP-OMe additive.

Fig. 4 displays the relation between frictional torque and time at succeeding loads beginning from 98 N experimental load. For the base lube, frictional torque increases slowly up to 1078 N load and thereafter increases abruptly due to failure of the tribofilm.





Scheme 1 Synthesis of tetrahydropyrazolopyridine derivatives.

Thus, base oil alone can sustain the load only up to 1078 N. It is noticeable that for ZDDP 0.25% w/v concentration is not compatible with increasing the load-bearing capacity of base lube. On the other hand, for the synthesized additives a sharp increase in frictional torque is noted at much higher loads, THPP-H (2450 N), THPP-Me (2548 N) and THPP-OMe (3038 N).

**Table 1** Molecular structures, IUPAC names, abbreviations and characterizations of the tetrahydropyrazolopyridine derivatives (THPP-H, THPP-Me, THPP-OMe)

S. no.	Structure	IUPAC name and abbreviation	Characterization
1		3,5-Dimethyl-4-phenyl-1,4,7,8-tetrahydropyrazolo[3,4- <i>b</i> :4',3'- <i>e</i> ]pyridine, (THPP-H)	Melting point 240–242 °C <sup>1</sup> H NMR (500 MHz, DMSO) δ 7.52–7.50 (2H, d), 7.15–7.13 (1H, d), 6.94 (2H, s), 4.62 (1H, s), 1.80 (6H, s). <sup>13</sup> C NMR (126 MHz, DMSO) δ 161.92, 143.71, 140.46, 128.24, 127.97, 125.93, 104.45, 32.81, 10.88.
2		3,5-Dimethyl-4-(4-methylphenyl)-1,4,7,8-tetrahydropyrazolo[3,4- <i>b</i> :4',3'- <i>e</i> ]pyridine, (THPP-Me)	Melting point 242–244 °C <sup>1</sup> H NMR (500 MHz, DMSO) δ 7.22–7.21 (2H, d), 7.06–7.03 (2H, d), 4.93 (1H, s), 2.11 (3H, s), 1.80 (6H, s). <sup>13</sup> C NMR (126 MHz, DMSO) δ 159.92, 140.93, 137.36, 134.87, 129.34, 127.75, 125.04, 124.52, 102.20, 30.50, 18.63, 9.88.
3		3,5-Dimethyl-4-(4-methoxyphenyl)-1,4,7,8-tetrahydropyrazolo[3,4- <i>b</i> :4',3'- <i>e</i> ]pyridine, (THPP-OMe)	Melting point 185–186 °C <sup>1</sup> H NMR (500 MHz, DMSO) δ 7.04–7.02 (2H, d), 6.78–6.76 (2H, d), 4.75 (1H, s), 3.68 (3H, s), 2.07 (6H, s). <sup>13</sup> C NMR (126 MHz, DMSO) δ 160.71, 156.81, 139.42, 134.80, 128.00, 112.75, 103.91, 54.43, 31.55, 9.96.



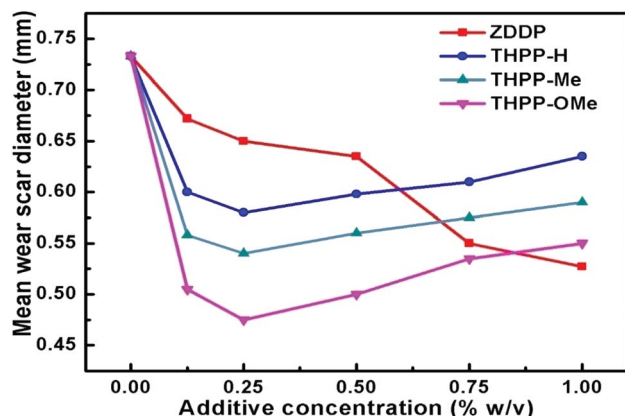


Fig. 1 Deviation in mean wear scar diameter with the concentration of different tetrahydropyrazolopyridine additives in PO at 392 N applied load for 60 min test.

Thus, the developed tribochemical film is much stronger to bear the load when THPP-OMe is applied as an additive.

The frictional power loss ( $P$ )<sup>37</sup> for different tetrahydropyrazolopyridine additives, collected in Table 2 has been calculated using the given eqn (1). The details are given in (ESI-3†).

$$P = 2.07 \times \mu \times 10^{-3} \text{ (W)} \quad (1)$$

where,  $\mu$  = coefficient of friction

$$1 \text{ kW h} = 3.6 \text{ MJ} \quad (2)$$

The PO shows highest power consumption (0.7064 MJ) as compared to the other additives, ZDDP (0.6296 MJ), THPP-H (0.6183 MJ), THPP-Me (0.5200 MJ) and THPP-OMe (0.4264 MJ). The highest percentage reduction in  $P$  was observed in case of THPP-OMe additive, 39.64%. Consequently, among all the tested additives, THPP-OMe additive saves substantial energy.

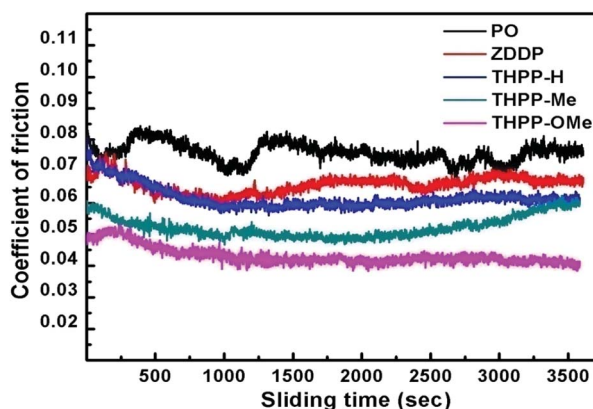


Fig. 2 Variation of the coefficient of friction with sliding time in the presence of different tetrahydropyrazolopyridine additives (0.25% w/v) in PO: load, 392 N; sliding speed, 1200 rpm; temperature, 75 °C; test duration, 60 min.

### 3.2. Surface examination of the wear scar

The worn surface has been examined by SEM and AFM (contact mode) after tribological test ASTM D4172. The SEM images of worn surface on steel ball in the presence of blank lubricant and its blends with tetrahydropyrazolopyridines (0.25% w/v) are shown in Fig. 5. The size of wear scar and its smoothness are directly related to the relative tribological performance of the synthesized additives. Thus, severely damaged wear scar surface for plain paraffin oil while substantially smoothed surface in case of THPP-OMe may be arguably discussed.

The AFM of the worn surface was performed after the antiwear test. The obtained data for surface roughness variables of wear scars on steel ball are displayed in Fig. 6 together with their 3D AFM figures.

The roughness parameters, root mean square area ( $S_q$ ) and root mean square line roughness ( $R_q$ ) were found to be very high ( $S_q = 674 \text{ nm}$ ,  $R_q = 670 \text{ nm}$ ) for the blank oil. A huge reduction in these values is marked in the presence of additives THPP-OMe ( $S_q = 46.98 \text{ nm}$ ,  $R_q = 37.41 \text{ nm}$ ), THPP-Me ( $S_q = 59.36 \text{ nm}$ ,  $R_q = 59.18 \text{ nm}$ ), THPP-H ( $S_q = 124.77 \text{ nm}$ ,  $R_q = 120.13 \text{ nm}$ ). The above-mentioned values of  $S_q$  and  $R_q$  validate the order of activity obtained from tribological data.

### 3.3. Energy dispersive X-ray spectroscopy (EDX)

The EDX analysis of wear scar in the presence of plain oil and its admixtures with tetrahydropyrazolopyridines has been performed after the antiwear test for elemental characterization of the tribofilm. Fig. 7 shows the EDX spectra of base lube and its admixture with THPP-OMe. Presence of nitrogen as the heteroatom can be easily seen in Fig. 7(b), emphasizing its contribution during the development of tribofilm.

### 3.4. X-ray photoelectron spectroscopy (XPS)

The deconvoluted XPS spectra of C 1s, N 1s, O 1s and Fe 2p of the tribofilm formed on the wear scar surface in the presence of THPP-OMe after following ASTM D4172 standards are displayed in Fig. 8.

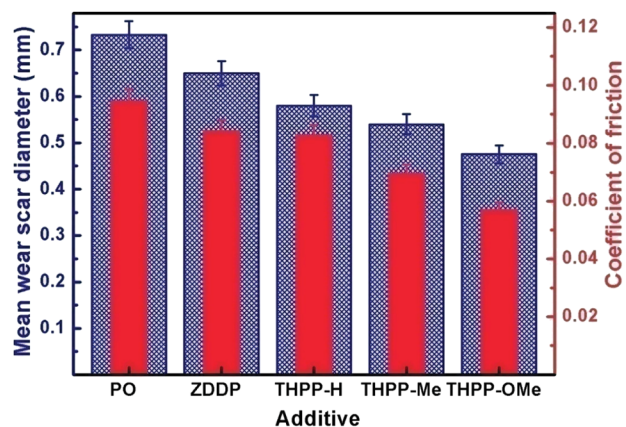


Fig. 3 Variation of mean wear scar diameter and coefficient of friction in the presence of tetrahydropyrazolopyridine additives in PO: load, 392 N; sliding speed, 1200 rpm; temperature, 75 °C; test duration, 60 min; concentration of additives, 0.25% w/v.





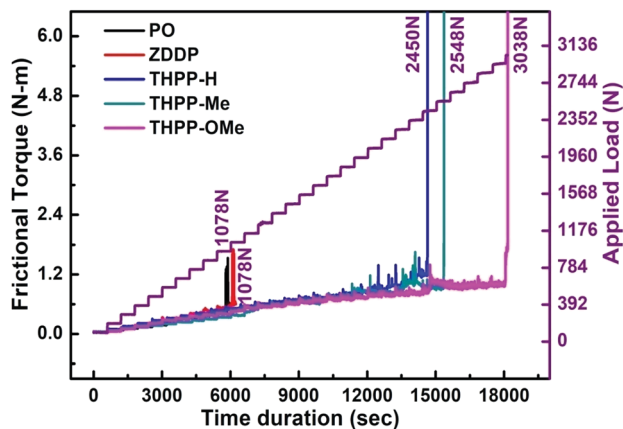


Fig. 4 Alteration of frictional torque with stepwise loading and time for different tetrahydropyrazolopyridine additives: sliding speed, 600 rpm; temperature, 75 °C; concentration of additives, 0.25% w/v.

The core-level spectrum of C 1s, Fig. 8(a) exhibits two peaks at 284.5, 285.1 eV binding energies corresponding to C-C/C=C, C-O/C-N bonds respectively.<sup>8,38,39</sup> Fig. 8(b) shows core-level spectrum of O 1s

indicating three peaks with binding energies 529.8, 532.1 and 533.5 eV which could be correlated with Fe-O/Fe<sub>2</sub>O<sub>3</sub>, C-O, C-O-C moieties respectively.<sup>40–42</sup> The N 1s spectrum is illustrated in Fig. 8(c). The presence of only one peak identified at 399.9 eV could be accorded with -N=C/-N-C- group.<sup>10</sup> The binding energies of Fe 2p at 710.8 eV (Fig. 8(d)) and O 1s at 529.8 eV (Fig. 8(b)) together indicate the formation of iron oxides FeO and Fe<sub>2</sub>O<sub>3</sub> confirming oxidation of steel surface iron during rubbing process.<sup>43</sup> Thus, it may be inferred that the additive adsorbed on the steel surface through heteroatoms has decomposed under tribo conditions to form a complex tribofilm along with the mixture of FeO/Fe<sub>2</sub>O<sub>3</sub> and rendered active participation in exceeding lubricating behavior.

### 3.5. Tribochemistry and proposed mechanism for triboaction

Based on tribological tests, it may be established that tetrahydropyrazolopyridine formulations prove to be extremely tribochemically active. The AFM and SEM results corroborate the experimental data for the relative activity of different additives. The energy dispersive X-ray analysis provides sufficient

Table 2 Loss of frictional power measured for different additives at the concentration, 0.25% (w/v) in PO

S. no.	Additives	Power consumption (MJ)	Reduction in power consumption	% reduction in power consumption
1	PO	0.7064	—	—
2	ZDDP	0.6296	0.0768	10.87
3	THPP-H	0.6183	0.0881	12.47
4	THPP-Me	0.5200	0.1864	26.39
5	THPP-OMe	0.4264	0.2800	39.64

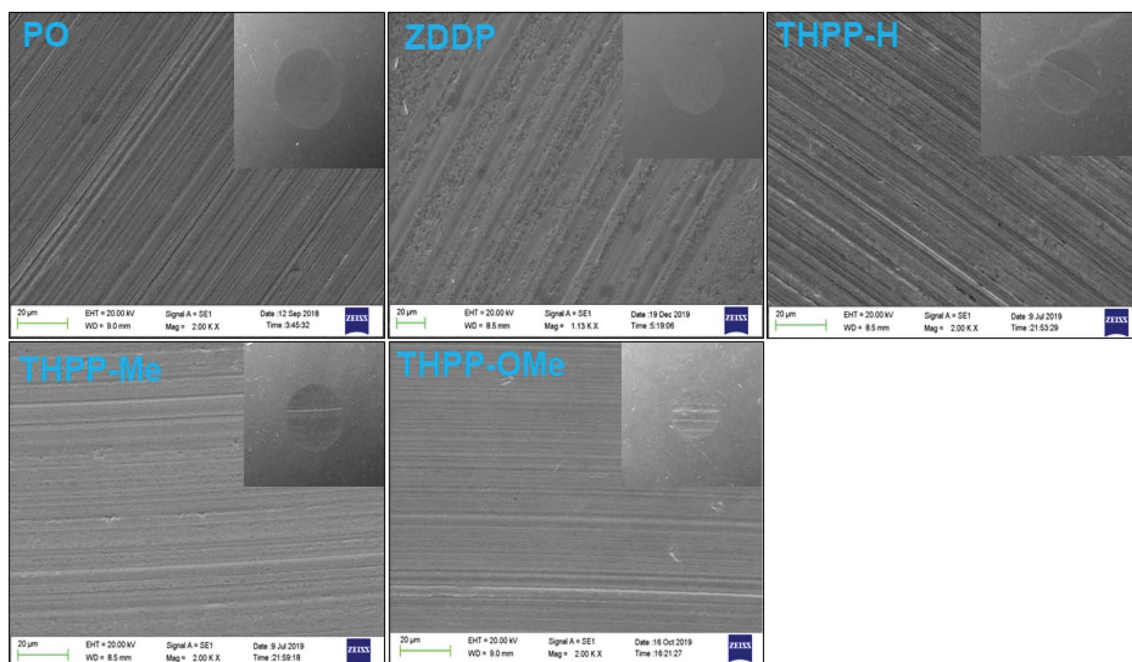


Fig. 5 SEM images (inset: full view of wear scar at 100 $\times$ , wear scar surface at 2.00k $\times$  magnification) of the worn steel surface lubricated with PO with or without tetrahydropyrazolopyridine additives (0.25% w/v) for 60 min test at 392 N applied load.



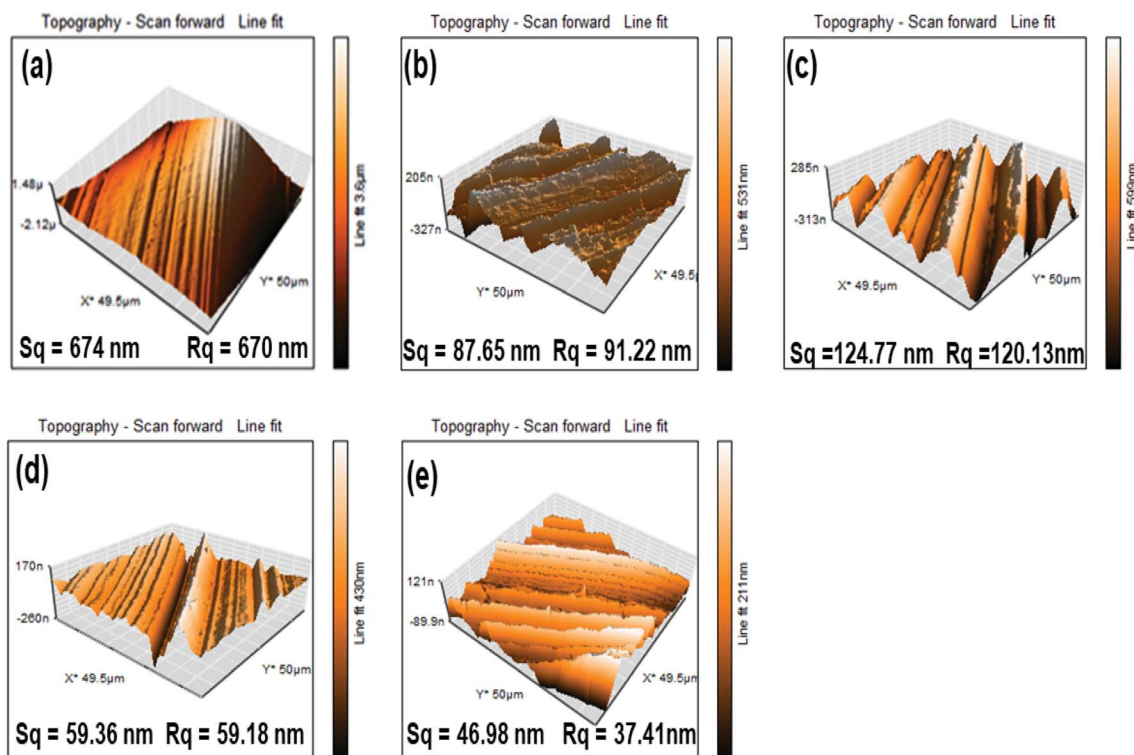


Fig. 6 3D AFM images of the wear scar surface in the presence of PO with or without different tetrahydropyrazolopyridine additives (0.25% w/v) for 60 min test duration at 392 N applied load (a) PO, (b) ZDDP, (c) THPP-H, (d) THPP-Me and (e) THPP-OMe.

evidence in support of heteroatoms present on the tribo-surface. A thin chemical film is formed under the tribo-test condition because of additive decomposition and interaction of the decomposed products with the mating surfaces. The tenacious film keeps the proximal surfaces away from each other and therefore, friction and wear are greatly reduced.

### 3.6. DFT calculations

The DFT calculations have been conducted to observe the effect of various substituents on the inherent framework of tetrahydropyrazolopyridine towards antiwear lubricating properties.

An endeavour has been made to correlate the test results with the molecular structures of the synthesized additives. Fig. 9 displays the optimized structures of the synthesized tetrahydropyrazolopyridine additives THPP-OMe, THPP-Me, THPP-H. At first, the additive molecules tend to undergo physical or chemical adsorption on the steel ball surface *via* their polar ends followed by their chemical interaction at the surface. Frontier Molecular Orbital (FMO) theory, may be ensued to give the mechanism of tribological behavior. The quantum chemical variables like total energy, the energy of highest occupied and lowest unoccupied molecular orbitals ( $E_{\text{HOMO}}$  and  $E_{\text{LUMO}}$ ) and

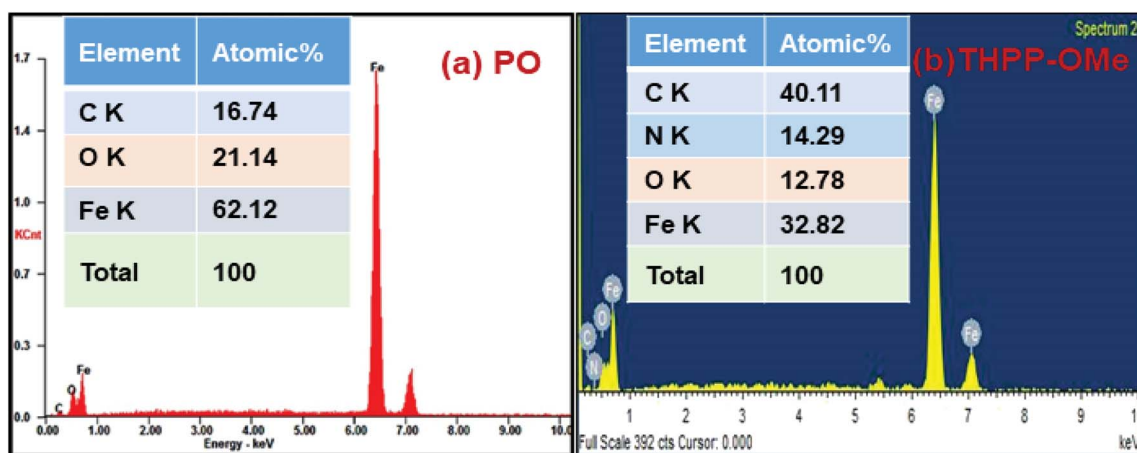


Fig. 7 EDX spectra of worn surface lubricated with (a) PO and (b) THPP-OMe.



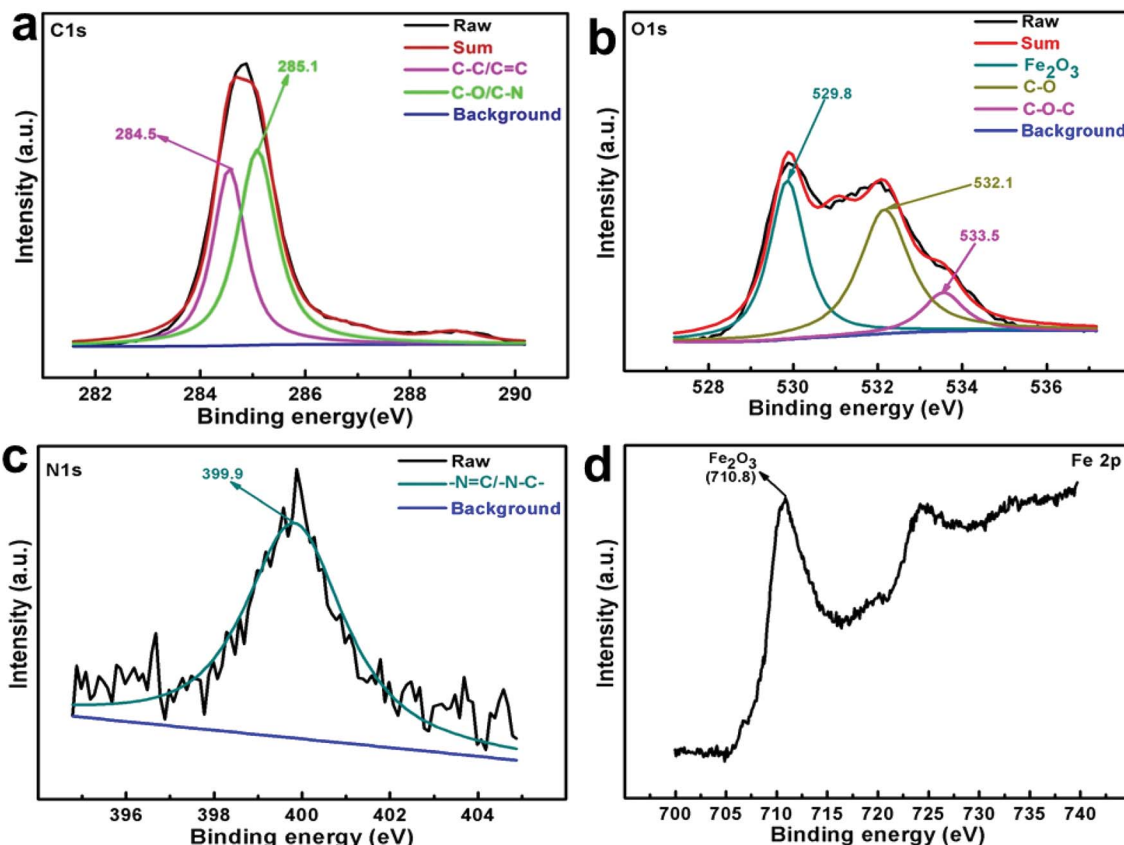


Fig. 8 XPS spectra of tribochemical film formed on worn steel surface lubricated with the THPP-OMe additive (0.25% w/v) at 392 N applied load for 60 min test duration in PO. (a) C 1s (b) O 1s (c) N 1s and (d) Fe 2p.

their energy gap ( $\Delta E = E_{\text{LUMO}} - E_{\text{HOMO}}$ ) are given in Table 3. These variables have been used to justify the reactivity of the additive molecules.

In accordance with the Hartree-Fock theorem,<sup>44</sup> the energies of frontier molecular orbitals are shown by:

$$I = -E_{\text{HOMO}};$$

$$A = -E_{\text{LUMO}}$$

where  $I$  and  $A$  correspond to the ionization potential and the electron affinity respectively and are depicted in Table 3.

The absolute electronegativity ( $\chi$ ) is given as:

$$\chi = (I + A)/2$$

The global hardness ( $\gamma$ ) is equal to:

$$\gamma = (I - A)/2$$

When metal (iron) and additive come in close proximity to each other, electron flows from lower  $\chi$  (additive) to higher  $\chi$  (iron) values until chemical potentials become equal.

The global softness ( $\sigma$ ) is defined as:

$$\sigma = 1/\gamma$$

Global softness ( $\sigma$ ) gives information about the reactivity of a compound.

Based on the hardness-softness concept, it may be stated that the highest value for  $\Delta E$  corresponds to highest stability index showing hard or inert behavior in a chemical reaction; on the other hand, its lowest value designates the lowest stability index accompanied with soft or easily polarized behavior. The soft additive with the smallest energy gap  $\Delta E$  is anticipated to show the maximum capability of adsorption and accordingly, it would be the most tribologically active additive. It is apparent from Table 3 that additive (THPP-OMe) is having the lowest value for  $\gamma$  and the highest for  $\sigma$ . Based on these parameters, the ascending order of tribological performance of the synthesized additives may be expressed as:



### 3.7. Structure-activity relationship

The tribological data achieved for different tetrahydropyrazolopyridines may be correlated with their corresponding structures. Structurally, a tetrahydropyrazolopyridine moiety has a pyridine ring fused with two pyrazole rings on either side. It may



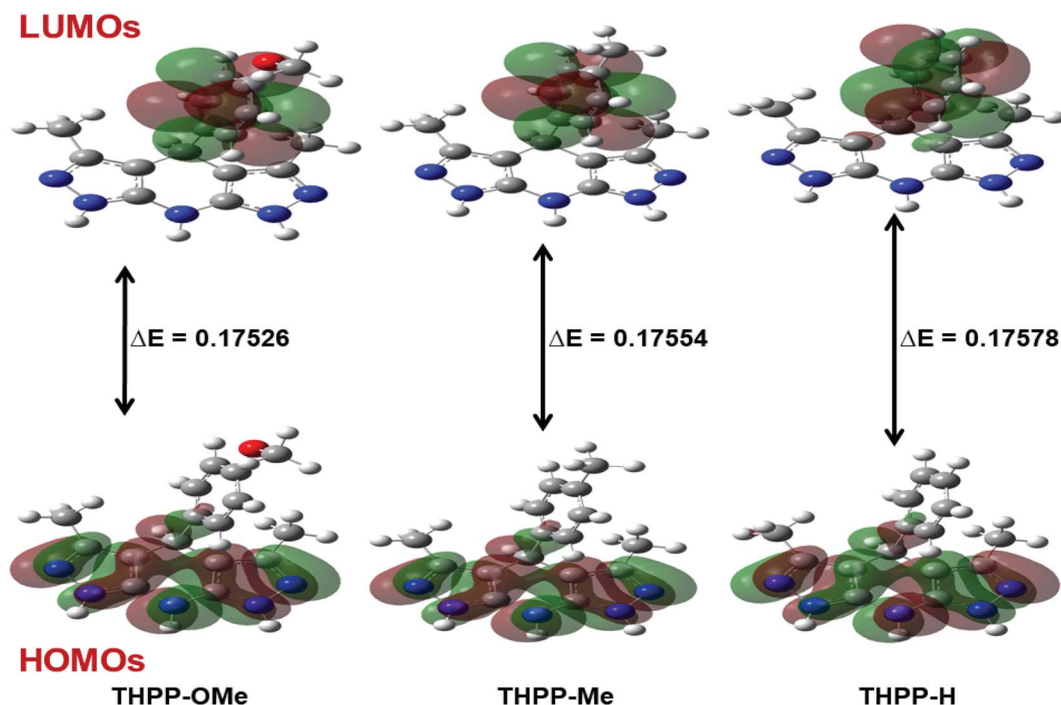


Fig. 9 Frontier Molecular Orbitals (HOMO and LUMO) of different tetrahydropyrazolopyridine additives with their  $\Delta E$  values.

Table 3 Quantum chemical parameters of tetrahydropyrazolopyridine antiwear additives by B3LYP/3-21G + \*

S. no.	Additives	Total energy (a.u.)	$E_{\text{HOMO}}$ (Hartree-Fock)	$E_{\text{LUMO}}$ (Hartree-Fock)	$\Delta E$ (Hartree-Fock)	$I$	$A$	$\chi$	$\gamma$	$\sigma$
1	Fe <sub>5</sub> (ref. 45)		-0.18651	-0.06420	0.12231	0.18651	0.06420	0.12535	0.06115	16.35322
2	THPP-OMe	-963.67	-0.20469	-0.02943	0.17526	0.20469	0.02943	0.11706	0.08763	11.41162
3	THPP-Me	-888.86	-0.20413	-0.02859	0.17554	0.20413	0.02859	0.11636	0.08777	11.39341
4	THPP-H	-849.75	-0.20529	-0.02951	0.17578	0.20529	0.02951	0.11740	0.08789	11.37786

get adsorbed on the steel ball surface *via* nitrogens of the pyrazoles and the pyridine ring. All the nitrogens being present in a delocalized system are engaged in surface adsorption. The relative performance of different additives is guided by the nature of substituents attached to the benzene ring at the 4<sup>th</sup> position of the pyridine group. As discussed above, the best activity is displayed by methoxy analogue (THPP-OMe) followed by methyl (THPP-Me) and then (THPP-H). The observed order reflects that the electron density on the fused rings has decreased accordingly. The +R effect of methoxy group and +I effect of the methyl group have been instrumental in increasing the electron-donating tendency of the corresponding tetrahydropyrazolopyridines.

## 4. Conclusions

(1) The tetrahydropyrazolopyridine additives were synthesized and characterized by NMR spectroscopy.

(2) The studied additives having zero SAPs contents show very high tribological activity at all the tested concentrations. The maximum activity is observed at a very low concentration, 0.25% w/v.

(3) Based on antiwear and load ramp tests at 0.25% w/v concentration, the activity of various additives could be established as:



(4) Morphological investigations of the wear scar surface authenticate the relative tribological activity.

(5) The DFT calculations verify the experimentally found data.

(6) The EDX analysis of the wear scar surface shows the presence of heteroatoms, nitrogen and oxygen confirming adsorption of different additives on the steel surface.

(7) XPS spectra of the wear scar surface confirm that tribochemical film is made up of decomposed products of the additive along with iron oxides.

## Conflicts of interest

There is no conflict of interest.





## Acknowledgements

One of the authors, Kavita acknowledge to Council of Scientific & Industrial Research (CSIR), India for financial support. Authors are grateful to the Incharge of Central Instrument Facility Centre (CIFC) – IIT (BHU), Varanasi for NMR and SEM with EDX services.

## Notes and references

- 1 S. C. Tung and M. L. McMillan, *Tribol. Int.*, 2004, **37**, 517–536.
- 2 S. M. Hsu, *Tribol. Int.*, 2004, **37**, 553–559.
- 3 M. D. Bermúdez, A. E. Jiménez, J. Sanes and F. J. Carrión, *Molecules*, 2009, **14**, 2888–2908.
- 4 M. K. A. Ali, H. Xianjun, L. Mai, C. Bicheng, R. F. Turkson and C. Qingping, *Wear*, 2016, **364**, 270–281.
- 5 B. Kumar, J. Kuntail, D. K. Verma, R. B. Rastogi and I. Sinha, *J. Mol. Liq.*, 2019, **289**, 111171.
- 6 Kalyani, V. Jaiswal, R. B. Rastogi and D. Kumar, *RSC Adv.*, 2014, **4**, 30500–30510.
- 7 Kalyani, R. B. Rastogi and D. Kumar, *ACS Sustainable Chem. Eng.*, 2016, **4**, 3420–3428.
- 8 D. K. Verma, B. Kumar, Kavita and R. B. Rastogi, *ACS Appl. Mater. Interfaces*, 2018, **11**, 2418–2430.
- 9 J. Wu, X. Huang, K. Berglund, X. Lu, X. Feng, R. Larsson and Y. Shi, *Compos. Sci. Technol.*, 2018, **162**, 86–92.
- 10 V. Jaiswal, S. R. Gupta, R. B. Rastogi, R. Kumar and V. P. Singh, *J. Mater. Chem. A*, 2015, **3**, 5092–5109.
- 11 B. H. Kim, J. C. Jiang and P. B. Aswath, *Wear*, 2011, **270**, 181–194.
- 12 A. M. Barnes, K. D. Bartle and V. R. A. Thibon, *Tribol. Int.*, 2001, **34**, 389–395.
- 13 P. Njiwa, C. Minfray, T. Le Mogne, B. Vacher, J. M. Martin, S. Matsui and M. Mishina, *Tribol. Lett.*, 2011, **44**, 19–30.
- 14 H. Spikes, *Lubr. Sci.*, 2008, **20**, 103–136.
- 15 M. K. A. Ali, H. Xianjun, L. Mai, C. Qingping, R. F. Turkson and C. Bicheng, *Tribol. Int.*, 2016, **103**, 540–554.
- 16 H. Xie, B. Jiang, J. He, X. Xia and F. Pan, *Tribol. Int.*, 2016, **93**, 63–70.
- 17 F. U. Shah, S. Glavatskih and O. N. Antzutkin, *ACS Appl. Mater. Interfaces*, 2009, **1**, 2835–2842.
- 18 B. Bhushan, J. N. Israelachvili and U. Landman, *Nature*, 1995, **374**, 607.
- 19 S. V. Didziulis, *Langmuir*, 1995, **11**, 917–930.
- 20 J. Lara, T. Blunt, P. V. Kotvis, A. Riga and W. T. Tysoe, *J. Phys. Chem. B*, 1998, **102**, 1703–1709.
- 21 H. Kamano and H. Koshima, *US Pat.*, 8,841,242 B2, 2014.
- 22 Z. He, W. Rao, T. Ren, W. Liu and Q. Xue, *Tribol. Lett.*, 2002, **13**, 87–93.
- 23 X. Xu, Y. Wan and L. Cao, *Wear*, 2000, **241**, 41–46.
- 24 J. Li, T. Ren, H. Liu, D. Wang and W. Liu, *Wear*, 2000, **246**, 130–133.
- 25 L. Xiong, Z. He, S. Han, J. Tang, Y. Wu and X. Zeng, *Tribol. Int.*, 2016, **104**, 98–108.
- 26 G. Yang, J. Zhang, S. Zhang, L. Yu, P. Zhang and B. Zhu, *Tribol. Int.*, 2013, **62**, 163–170.
- 27 M. Desanker, X. He, J. Lu, P. Liu, D. B. Pickens, M. Delferro, T. J. Marks, Y. W. Chung and Q. J. Wang, *ACS Appl. Mater. Interfaces*, 2017, **9**, 9118–9125.
- 28 M. D. Avilés, F. J. Carrión-Vilches, J. Sanes and M. D. Bermúdez, *Tribol. Lett.*, 2019, **67**, 26.
- 29 P. S. Bakshi, R. Gusain, M. Dhawaria, S. K. Suman and O. P. Khatri, *RSC Adv.*, 2016, **6**, 46567–46572.
- 30 J. Wu, L. Mu, X. Feng, X. Lu, R. Larsson and Y. Shi, *Adv. Mater. Interfaces*, 2019, **6**, 1–8.
- 31 L. Zhang, D. Feng and B. Xu, *Tribol. Lett.*, 2009, **34**, 95–101.
- 32 R. Gusain, P. Gupta, S. Saran and O. P. Khatri, *ACS Appl. Mater. Interfaces*, 2014, **6**, 15318–15328.
- 33 D. K. Verma, Kalyani, V. Jaiswal and R. B. Rastogi, *Tribol. Trans.*, 2019, **62**, 283–294.
- 34 V. Jaiswal, Kalyani, R. B. Rastogi and R. Kumar, *J. Mater. Chem. A*, 2014, **2**, 10424–10434.
- 35 M. Dabiri, P. Salehi, M. Koohshari, Z. Hajizadeh and D. I. MaGee, *Arkivoc*, 2014, 204–214.
- 36 S. Dapprich, A. D. Daniels, M. C. Strain, O. Farkas, D. K. Malick, A. D. Rabuck, K. Raghavachari, J. B. Foresman, J. V. Qrtiz, Q. Cui and A. G. Baboul, *Gaussian 03, revision C.01*, Gaussian, Inc., Wallingford, CT, 2004.
- 37 S. S. Rawat, A. P. Harsha, S. Das and A. P. Deepak, *Tribol. Trans.*, 2019, 1–11.
- 38 B. Kumar, D. K. Verma, A. K. Singh, Kavita, N. Shukla and R. B. Rastogi, *Compos. Interfaces*, 2019, 1–18.
- 39 F. Sordello, G. Zeb, K. Hu, P. Calza, C. Minero, T. Szkopek and M. Cerruti, *Nanoscale*, 2014, **6**, 6710–6719.
- 40 G. Yang, Z. Zhang, G. Li, J. Zhang, L. Yu and P. Zhang, *J. Tribol.*, 2011, **133**, 1–7.
- 41 G. Yang, J. Zhao, L. Cui, S. Song, S. Zhang, L. Yu and P. Zhang, *RSC Adv.*, 2017, **7**, 7944–7953.
- 42 V. Kumar, D. Bano, D. K. Singh, S. Mohan, V. K. Singh and S. H. Hasan, *ACS Sustainable Chem. Eng.*, 2018, **6**, 7662–7675.
- 43 J. Zhou, Z. Wu, Z. Zhang, W. Liu and H. Dang, *Wear*, 2001, **249**, 333–337.
- 44 P. Mourya, P. Singh, A. K. Tewari, R. B. Rastogi and M. M. Singh, *Corros. Sci.*, 2015, **95**, 71–87.
- 45 W. Huang, Y. Tan, B. Chen, J. Dong and X. Wang, *Tribol. Int.*, 2003, **36**, 163–168.

